Pure Appl. Chem.,Vol. 81, No. 9, pp. 1603–1614, 2009.
doi:10.1351/PAC-CON-08-11-09

Modification of molecular organization of polymers by gas sorption: Thermodynamic aspects and industrial applications*

Séverine A. E. Boyer[1], Takeshi Yamada[2], Hirohisa Yoshida[3], and Jean-Pierre E. Grolier[4,‡]

[1]Centre for Material Forming, CEMEF (CNRS UMR 7635), Mines ParisTech, 06904 Sophia Antipolis, France; [2]Institute for Solid State Physics, The University of Tokyo, Kashiwa 277-8581, Japan; [3]Graduate School of Environmental Science, Tokyo Metropolitan University, Hachiouji Tokyo 198-0397, Japan; [4]Laboratory of Thermodynamics of Solutions and Polymers, Blaise Pascal University, 63177 Aubière, France

Abstract: In polymer science, gas–polymer interactions play a central role for the development of new polymeric structures for specific applications. This is typically the case for polymer foaming and for self-assembling of nanoscale structures where the nature of the gas and the thermodynamic conditions are essential to control. An important applied field where gas sorption in polymers has to be documented through intensive investigations concerns the (non)-controlled solubilization of light gases in the polymers serving, for example, in the oil industry for the transport of petroleum fluids.

An experimental set-up coupling a vibrating-wire (VW) detector and a *pVT* technique has been used to simultaneously evaluate the amount of gas entering a polymer under controlled temperature and pressure and the concomitant swelling of the polymer. Scanning transitiometry has been used to determine the interaction energy during gas sorption in different polymers; the technique was also used to determine the thermophysical properties of polymers submitted to gas sorption. The role of the pressurizing fluid has been documented in terms of the influence of pressure, temperature, and nature of the fluid.

Keywords: gas sorption; high pressure; polymers; scanning transitiometry; vibrating-wire technique.

INTRODUCTION

Polymers either as constitutive components of on-duty materials (such as seals, pipes, containers) or as essential intermediates for end-products (foams, insulating agents, templates) are in many applications submitted to high-pressure fluids, in particular, supercritical fluids. Whatever the state of the fluid (gaseous or supercritical), its sorption in the polymeric structure induces significant modifications of the molecular organization. Some undesirable modifications may generate possible destruction of the polymer matrix. For instance, in the petroleum industry, the transport of petroleum fluids is made using

*Paper based on a presentation at the 13th International Symposium on Solubility Phenomena and Related Equilibrium Processes (ISSP-13), 27–31 July 2008, Dublin, Ireland. Other presentations are published in this issue, pp. 1537–1614.

‡Corresponding author

flexible hosepipes, which structures contain extruded thermoplastic or rubber sheaths and reinforcing metallic armor layers. The thermoplastic polymers, like elastomers, may undergo sorption/diffusion phenomena, and a rupture of the thermodynamic equilibrium after a sharp pressure drop may eventually damage the polymer components; effectively, gas concentration in the polymer, with temperature gradients, causes irreversible "explosive" deterioration of the polymeric structures. This process manifests itself by cracks, blisters, or microstructures, like foams. This blistering phenomenon is usually termed "explosive decompression failure" (XDF) [1–4]. The resistance to such physical changes is related to the influence of different molecular interactions on the thermophysical properties of the polymer. The estimation of the gas sorption and of the concomitant polymer swelling as well as the measurement of the thermal effects associated with the gas–polymer interactions provide valuable and basic information for a better understanding of the polymer behavior in different applications, where temperature and pressure, in combination with supercritical fluid stress, may deeply affect the polymer stability and properties. However, high-pressure technology using gases plays an important role in materials nucleation. Particularly interesting are current developments and applications in soft matter science with typical modifications and tailoring of liquid crystals, colloids, and polymers including block copolymers, by means of supercritical gases [5–10]. In this respect, the thermodynamic investigation of di-block copolymers connecting incompatible polymers by covalent bonds is illustrative from both fundamental and applied aspects [11–14]. The synthesis of amphiphilic liquid crystal block copolymers consisting of hydrophilic polyethylene oxide (PEO) and hydrophobic polymethacrylate derivatives having side-chain liquid crystals which mesogen is azobenzene [PMA(Az)] has been recently reported [15]. The PEO_m-*b*-$PMA(Az)_n$ copolymers, where "*m*" and "*n*" are degrees of polymerization of PEO domain and PMA(Az) domain, respectively, form highly self-ordered PEO hexagonal-packed cylinder structures in the nanoscale in a wide range of volume fractions and give rise to four kinds of successive phase transitions, namely: melting of PEO crystal, glass transition of azobenzene moieties PMA(Az), liquid crystal transition from smectic C (SmC) phase to smectic A (SmA) phase and isotropic transition, respectively [15,19]. As an example of a typical application, Yung et al. have reported on the modification of the hexagonal-packed PEO cylinder structure by PEO homo-polymer blends in order to use the nanostructures as nanotemplates [20]. In fact, modification of nano-ordered structures formed by block copolymers is a key technology in nanoscience, and an important feature of self-ordered structures is their reorganization by modification of interface between the two components of di-block copolymers under the double effect of pressure and of the pressurizing fluid used to pressurize. Then, control of the undesirable as well as desirable modifications of polymers by high-pressure fluids necessitates the most appropriate high-pressure experiments requiring specific experimental techniques. Effectively, understanding and controlling the above modifications imply documented quantitative information on thermophysical properties of not only native materials but also of the materials under pressure in the presence and absence of fluid (i.e., gas) sorption. Also, thermodynamic characterization of the different transitions undergone by the materials as well the energy of gas–polymer interactions is needed; furthermore, the amount of gas entering the polymeric materials has to be documented as well. In what follows, we give an account of recent developments in the ad hoc experimental techniques employed and on pertinent data obtained therefrom; a few examples serve to illustrate some technological/industrial applications.

EXPERIMENTAL TECHNIQUES

New techniques based on fundamental thermodynamic principles allow us to modify in depth the molecular organization of polymeric materials while following, controlling, or monitoring the possible modifications generated in the polymeric materials when submitted to temperature and/or pressure scans, in the presence or absence of more or less reacting fluids used as pressurizing fluids. The thermodynamic control of the different processing steps includes measurement or determination of gas solubility, polymer swelling, gas–polymer interactions, thermophysical properties of polymers under or in

absence of gas sorption, as well as the thermal characterization of state transitions (melting/crystallization and glass transitions). Experimental measurements deal with polymers like polyethylenes (PEs), poly(vinylidene fluoride) (PVDF), amphiphilic di-block copolymers, and pressurizing fluids like carbon dioxide (CO_2), nitrogen (N_2), or mercury (Hg). Two main types of coupled techniques that have been developed are subsequently described: a weighing-expansion set-up to simultaneously estimate the amount of gas absorbed in a polymer and the concomitant swelling of the polymer, and a *pVT*-calorimetric apparatus to fully characterize the thermodynamic gas–polymer interactions.

Gas solubility and polymer swelling concomitant determination

The technique [21] consists in determining simultaneously in situ in a high-pressure cell (the measuring cell) the quantity of gas entering into a polymer sample and the change in volume, i.e., the swelling, of the polymer due to the sorption of gas. This original concept combines in the high-pressure cell two techniques, a weigh sensor based on the principle of a vibrating wire (VW) through which the polymer sample is suspended, and a pressure decay *pVT* technique, controlling the amount and the pressure of gas introduced in the cell. The VW sensor is employed as a force sensor to weigh the polymer during the sorption; the buoyancy force exerted by the pressurized gas on the polymer depends on the volume change, ΔV_{pol}, of the polymer due to the gas sorption. Actually, the polymer sample, in complete immersion in the gas contained in the high-pressure cell, is placed in a holder. This holder, made of nonmagnetic metal, is suspended by a thin (diameter 25 μm; length 30 mm) tungsten wire in such a way that the wire is positioned at the center of a high magnetic field generated by a magnet placed across the high-pressure cell (Fig. 1). The magnet made of a samarium-cobalt alloy is constituted of two square parts placed symmetrically in tight contact on both sites of the high-pressure measuring cell. The vibration of the fine tungsten wire is activated by means of an electric circuitry and electronically controlled; then, the natural period of vibration of the wire can be measured with high precision. This vibration period is directly related to the suspended sample. The *pVT* technique consists of introducing in the measuring cell containing the suspended polymer sample successive amounts of the gas, initially kept in a reservoir cell, through a calibrated high-pressure transfer cell (Fig. 1). The three cells are all placed inside the same thermostat constituted of a cylindrical stainless steel block heated by thermal screens; this thermostat is sitting inside a large aluminum vacuumed cylindrical container with a doubled (jacket) wall; the whole arrangement controls the temperature of the measuring cell within ±0.01 K. From the initial pressure p_i of the gas upon admission in the measuring cell, the pressure decay is then monitored until the final constant value p_f corresponding to the thermodynamic equilibrium for the gas–polymer system is reached. From the difference in pressure ($p_i - p_f$) and using the equation of state of the gas, the number of moles of gas n_{sol} solubilized in the polymer can be calculated after each gas injection. The experimental procedure is realized through a series of successive gas injections from the transfer cell to the measuring equilibrium cell until the polymer saturation is observed. The sets of pressures p_i and p_f recorded for each injection allow us to calculate through successive iterations [22] both the total mass m_{sol} of gas absorbed and the corresponding volume change ΔV_{pol} of the polymer sample. The iterative calculus utilizes two rigorous equations [21,22], one for the VW sensor, the other one for the *pVT* pressure decay method, which each contain the two unknowns m_{sol} and ΔV_{pol} which are related by the following relations:

$$m_{sol} = \rho_{gas}\,\Delta V_{pol} + [(\omega^2 - \omega_0^2)\,4L^2\,R^2\,\rho_S/\pi g + \rho(V_C - V_{pol})] \quad (1)$$

where ω_0 and ω are the natural angular frequency of the VW, respectively, in vacuum and under (gas) pressure, V_C the volume of the sample holder, while L, R, and ρ_S are, respectively, the length, radius, and density of the VW.

Relation 1 can be written as well in the following form:

$$m_{sol} = \rho_{gas}\,\Delta V_{pol} + d \tag{2}$$

where d depends only on the physical characteristics of the measuring system, that is essentially of the VW. As a matter of fact, the VW technique is more precise than the p-decay method since it does not generate the possible cumulative errors accompanying the successive gas injections along an absorption isotherm as the pVT technique. The main source of uncertainty comes from the term $\rho_{gas}\,\Delta V_{pol}$ in eq. 2, that is to say, the evaluation of the gas density and the change in volume. As a consequence, a procedure was proposed [23] to estimate the apparent solubility of the gas in the polymer and the associated volume change. This procedure is using the Sanchez–Lacombe equation of state (SL-EOS) to estimate the change in volume of the polymer at different temperatures and pressures. The VW sensor + pVT monitoring apparatus has been designed to determine in situ the amount of gas absorbed up to saturation in a polymer sample and the concomitant swelling of the polymer up to 100 MPa, from ambient temperature up to 473 K.

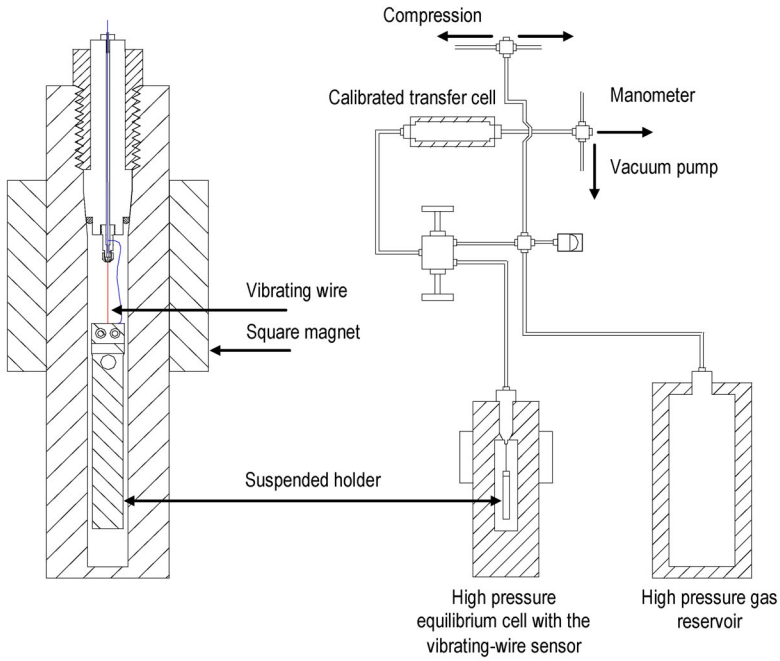

Fig. 1 Schematic representation of the coupled technique gas solubility-polymer swelling. On the left-hand side is a detailed view of the measuring high-pressure cell containing the polymer sample in its holder suspended by the VW.

Gas–polymer calorimetric investigation under different *pVT* conditions

Coupling of calorimetric measurements carried under the possible combinations of scanning the three thermodynamic variables p, V, and T has eventually yielded a now well-established very versatile technique, i.e., scanning transitiometry [24]. Practically, the technique utilizes the principle of differential heat flow calorimetry with which it is possible to operate under four thermodynamic situations where the perfectly controlled variation (or perturbation) of one of the three state variables (p, V, or T) is simultaneously recorded with the thermal effect resulting from the generated perturbation of the system under investigation [25]. The principle of scanning transitiometry [26] offers the possibility to scan, in the measuring calorimetric cell, one of the three independent thermodynamic variables (p, V, or T)

while keeping another one constant. During this scan, are recorded simultaneously in situ in the measuring cell, the variation of the (third) dependable variable (e.g., the mechanical output) and the calorimetric energy generated (e.g., the thermal output). From these two quantities associated to a given scan, two thermodynamic derivatives, mechanical and thermal, are thus determined; they perfectly characterize the evolution of the thermodynamic potential of the investigated system, particularly any transition or state change undergone induced by the variable scan. As illustrated in Fig. 2, making use of the rigorous Maxwell relations between thermodynamic derivatives it is possible to directly obtain the ensemble of the thermophysical properties; undoubtedly, this shows the potentiality of the technique. During measurements it is essential that the different scans be performed with sufficiently slow rates in order to keep the investigated system at equilibrium over the entire scan and that the (Mawxell) thermodynamic relations remain valid. In the present work, two different operating modes were used. On the one hand, the use of pressure as scanned variable along different isotherms while recording (vs. time t) simultaneously the associated thermal effect $(\delta Q/\mathrm{d}t)_T$ and the mechanical effect $(\partial V/\mathrm{d}t)_T$; on the other hand, the use of temperature as scanned variable along isobars while recording simultaneously the associated thermal effect $(\delta Q/\mathrm{d}t)_p$ and the mechanical effect $(\partial V/\mathrm{d}t)_P$.

In the case of the first mode, the straightforward thermodynamic relations [26]

$$\mathrm{d}H(T,p) = (\partial H/\partial T)_p \mathrm{d}T + (\partial H/\partial p)_T \mathrm{d}p \tag{3}$$

with

$$\mathrm{d}H(T,p) = \delta Q + V\mathrm{d}p \tag{4}$$

allow us to express finally that the thermal effect $q_T(p)$ along the scan is

$$q_T(p) = (\delta Q/\mathrm{d}t)_T = a[(\partial H/\partial p)_T - V] = aT(\partial S/\partial p)_T = -aT(\partial V/\partial T)_P = -aTV\alpha_p \tag{5}$$

where H, S, a, and α_p are, respectively, the enthalpy, the entropy, the pressure scanning rate, and the isobaric thermal expansion.

In addition, the associated mechanical effect $(\partial V/\mathrm{d}t)_T$, or equivalently $(\partial V/\partial p)_T$, allows us to obtain the isothermal compressibility κ_T.

Similarly in the second mode, from eqs. 3 and 4, at constant pressure (e.g., $\mathrm{d}p = 0$) one obtains for the thermal effect $q_p(T)$ an equation equivalent to eq. 3, C_p being the heat capacity

$$q_p(T) = b(\partial H/\partial T)_p = bC_p \tag{6}$$

In the same way as above, the mechanical output $(\partial V/\partial T)_P$ allows us to obtain the isobaric thermal expansion α_p.

The transitiometric technique can be utilized with fluids (gases and liquids) as well as with solid materials (polymers and metals); remarkably, measurements can be performed in the vicinity and above the critical point. Concretely, the investigated polymer samples are placed in ampoules; in fact, open mini-test tubes sitting in the transitiometric measuring cell in such a way that the sample is in direct contact with the pressurizing fluid. More details on the technique can be found elsewhere [27–29]. The transitiometers (from BGR TECH, Warsaw) used in the present work, built according to the above principle, can be operated over the respective following ranges of temperature and pressure 173 K < T < 673 K and 0.1 MPa < p < 200 MPa (or 400 MPa).

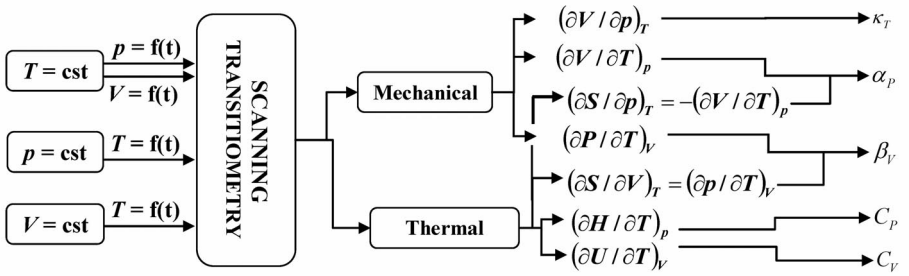

Fig. 2 Scheme of the scanning transitiometry showing the four possible thermodynamic modes with the respective associated thermal effects and mechanical effects as well as the corresponding different thermodynamic derivatives which deliver the four different pairs of thermophysical properties: the isobaric thermal expansion α_p, the isothermal compressibility κ_T, the isochoric thermal pressure coefficient β_V, the heat capacities at constant pressure and constant volume C_p and C_V.

RESULTS AND DISCUSSION

Several examples serve to illustrate the use of the above-described techniques for the investigation of the modifications undergone by polymers upon gas sorption. Two applications have been selected herein to document the major role of the nature of gases and the thermodynamic conditions to understand and eventually prevent or monitor such modifications. One application concerns the thermophysical properties of polymers used in the petroleum industry; the other one concerns the thermodynamic control of the formation of molecular self-assembled organizations at the polymer–liquid crystal interfaces in amphiphilic di-block copolymers.

Thermophysical properties of polymer saturated by gas sorption

As indicated in the Introduction, in order to understand and possibly prevent the blistering phenomena, a fundamental study, including a significant experimental part, has been carried out in particular to establish gas–polymer interactions in terms of gas solubility, polymer swelling, and induced polymer thermophysical properties [30]. The coupled technique VW + *pVT* method was used to determine the solubility of different gases (CO_2, N_2, CH_4) in different polymers [PEs, poly(methyl methacrylate) (PMMA), PVDF]. Figure 3 shows the results obtained for CO_2 and a medium-density polyethylene (MDPE).

Scanning transitiometry has been used to determine the gas–polymer interaction energy. Figure 4 shows, as an example, the thermal energy measured in the case of the CO_2 sorption in MDPE and in PVDF samples. Measurements have been made under either compression or decompression runs realized by pressure jumps Δp between 6 and 28 MPa. The most striking result is that CO_2–PVDF (exothermal) interactions are larger than CO_2–MDPE interactions for CO_2 pressures lower to 30 MPa, whereas above this pressure an inversion is observed with CO_2–MDPE interactions smaller than CO_2–PVDF interactions.

Scanning transitiometry has also been used to determine the isobaric thermal expansion α_p of different polymers. This thermophysical property is particularly important for industrial applications under extreme conditions of temperature and pressure. In this context, a study of different PEs of low, middle, and high densities (LDPE, MDPE, and HDPE, respectively) have been completed at several temperatures between 300 and 400 K and under different pressures up to 300 MPa. Extrapolation of these results allows us to obtain α_p for a PE supposedly totally crystallized [31], remarkably and very satisfactorily, the extrapolated value at atmospheric pressure is in very good agreement with the value calculated using the Pastine equation of state, which equation has the particularity to have been designed from crystallographic data.

The real advantage of using a differential detection between the two cells of a scanning transitiometer is the possibility to directly compare in identical conditions of temperature and pressure two polymer samples submitted to the same pressurizing gas. With the particular objective to examine the reactivity and behavior of two polymers under the very same gas, the isobaric thermal expansion $\alpha_{p(\text{global alpha})}$ of the gas-saturated polymers has been determined. Figure 5 shows the values of $\alpha_{p(\text{global alpha})}$ for the systems CO_2–MDPE and CO_2–PVDF obtained either through sorption or desorption as functions of pressure in the pressure range 0.1–90 MPa. The first meaningful result is that the $\alpha_{p(\text{global alpha})}$ isotherms for the two polymers saturated with CO_2 exhibit a minimum around 14–18 MPa for MDPE and 21–25 for PVDF, respectively, in contrast with what is observed in case the pressure-transmitting fluid is either Hg or N_2 for which no minimum is observed (see Fig. 5). The second interesting result is that above 30 MPa when the CO_2–MDPE interactions are energetically stronger than the CO_2–PVDF interactions, the $\alpha_{p(\text{global alpha})}$ is higher for MDPE than for PVDF. Such behavior confirms that the reactivity of CO_2 is chemically more "active" than (neutral) N_2 and than "inert" Hg, which is particularly marked in the vicinity of its critical point. Another important point of the results in Fig. 5, as observed in the case of PVDF, is that the values of $\alpha_{p(\text{global alpha})}$ obtained either under compression or decompression are similar, indicating a good reversibility of the phenomena of sorption/desorption. One notes also a practically identical evolution of $\alpha_{p(\text{global alpha})}$ when a given polymer is pressurized by either Hg or N_2 again in contrast with pressurization under CO_2.

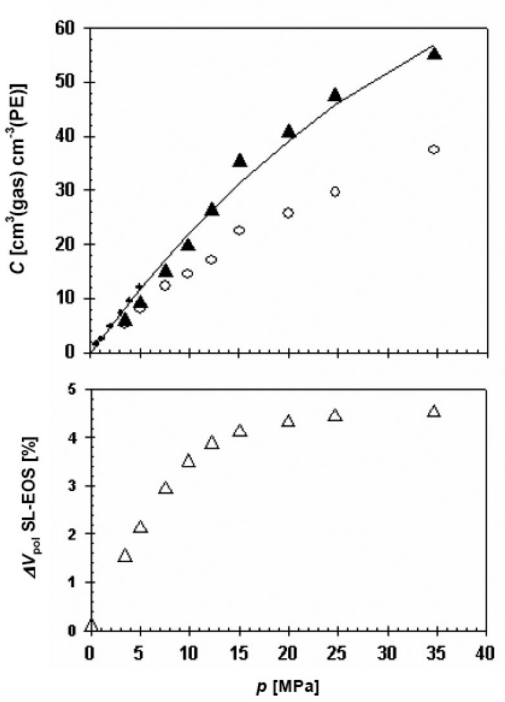

Fig. 3 Sorption of CO_2 in MDPE at 333 K as a function of pressure up to 35 MPa. The apparent concentrations C (cm^{-3} of CO_2/cm^{-3} of PE) are indicated by open circles. The corrected concentrations calculated from the polymer swelling ΔV_{pol} are indicated by full triangles; the values of ΔV_{pol} (open triangles in the diagram) have been calculated with the SL-EOS. Literature values (+) are from Kamiya et al. for LDPE at 308 K [*J. Polym. Sci., Part B: Polym. Phys.* **24**, 1525 (1986)].

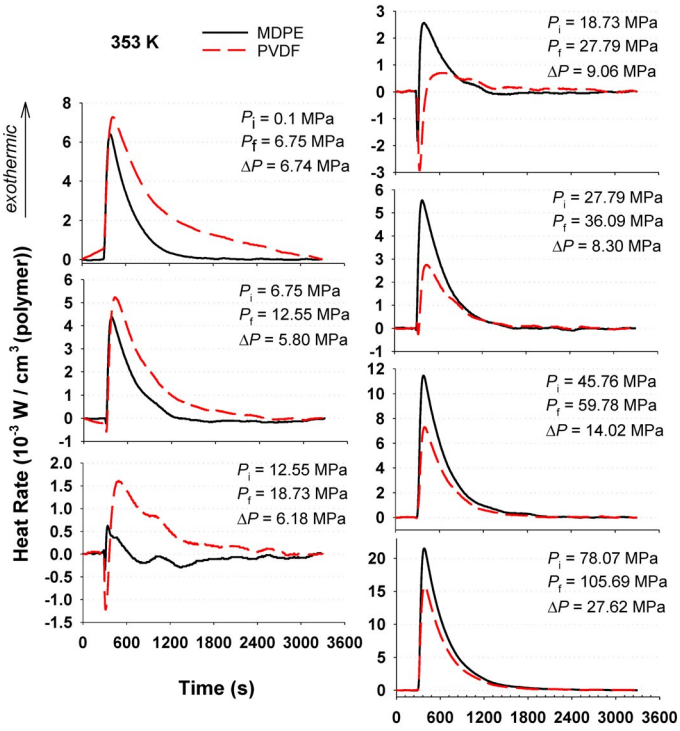

Fig. 4 Thermal energy of CO_2–polymer interactions at 353 K; comparison between the two polymers MDPE and PVDF. Measurements have been made under pressure jumps Δp, between initial pressures p_i and final pressures p_t respectively. The differential exothermal heat flows are of the order of a few mw per polymer cm^3.

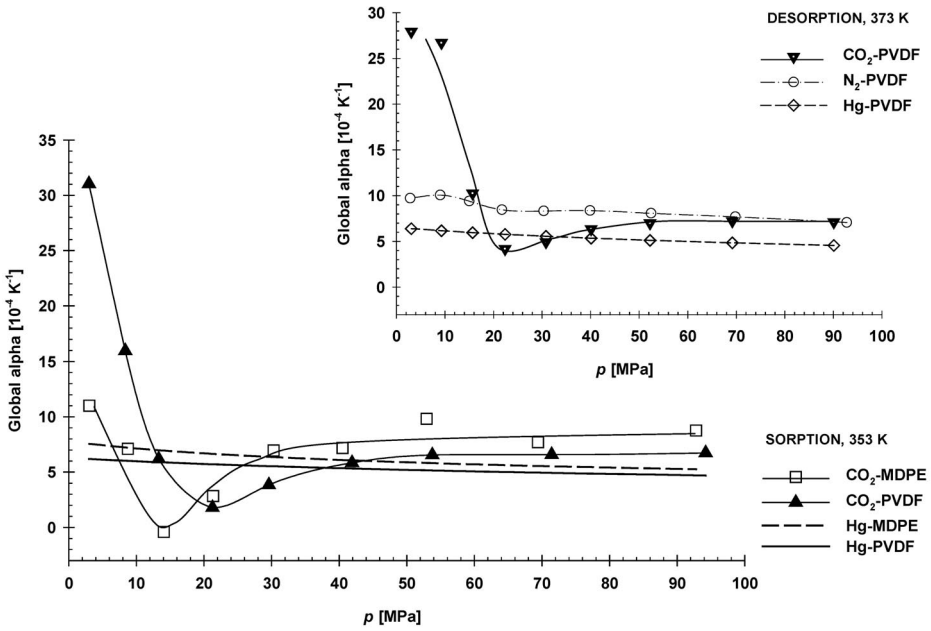

Fig. 5 Global isobaric thermal expansion $\alpha_{p(\text{global alpha})}$ for PVDF and MDPE samples submitted to high pressures transmitted either under compression (sorption) or decompression (desorption) of the three fluids CO_2, N_2, or Hg.

Role of high-pressure gas on molecular self-assembled organizations

The great variety of phases in liquid crystals is advantageously utilized in amphiphilic di-block copolymers in which the interface between the hydrophilic liquid crystal and the hydrophobic polymer moieties is the place where ordered nanostructures are developing by self-assembling in macroscopic spaces. As a matter of fact, the organization of these nanostructures can be perfectly controlled under pressure by modification of the interface depending on the nature of the pressurizing fluid, CO_2, N_2, or Hg. A systematic study has been conducted with di-block copolymers of the type PEO_m-*b*-$PMA(Az)_n$ comprising a hydrophilic PE oxide entity PEO and a hydrophobic methacrylate liquid crystal derivative with azobenzene mesogen groups PMA(Az). These copolymers PEO_m-*b*-$PMA(Az)_n$ where m and n are degrees of polymerization, generate at the interface between PEO and PMA(Az) moieties, well-ordered structures of one in the other depending on their respective volume fraction. The ordered structures can be of three different types: spheres, cylinders, or lamellae as illustrated in Fig. 6 for an AB-type di-block copolymer [A and B standing respectively for PEO and PMA(Az)]. Obtaining a given molecular organization of these structures as regards their type, size, and arrangement is directly controlled by the thermodynamic conditions, that is to say, p, T and the nature of the hydraulic fluid used to pressurize. In this respect, scanning transitiometry is well suited to document the role played by these parameters. To this end, the isotropic transition of the di-block copolymer at which well-defined self-organized nanoscale structures are forming is the main thermodynamic property to document. In the series of PEO_m-*b*-$PMA(Az)_n$ copolymers, PEO self-organized entities in the form of highly ordered periodic hexagonal-packed PEO cylinders are formed in the PMA domain by annealing at the isotropic state, showing then that controlling the phase changes at the interface allows tailoring of the nanoscale structures (Fig. 7). Scanning transitiometry has been used to evaluate the pressure dependence of the isotropic transition temperature T_{tr}, as well as the role of the nature of the pressurizing fluid. For this, the rigorous Clapeyron equation was advantageously used to document the pressure effect since this equation relates the slope (dT/dp) of the phase boundary on the p-T surface to the changes in volume ΔV_{tr} and enthalpy ΔH_{tr} at the transition as given by eq. 7

$$(dT/dp)_{tr} = T_{tr}\,\Delta V_{tr}/\Delta H_{tr} = \Delta V_{tr}/\Delta S_{tr} \tag{7}$$

where ΔS_{tr} is the change of entropy during the transition at temperature T_{tr}.

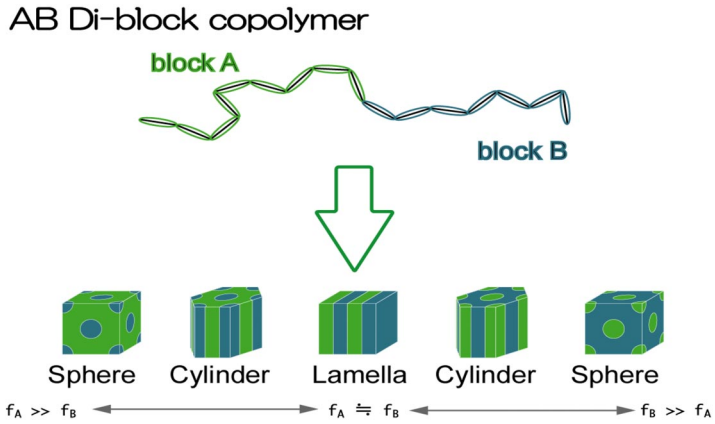

Fig. 6 Schematic representation of an AB di-block copolymer and display of possible ordered structures depending on the respective volume fractions f_A and f_B.

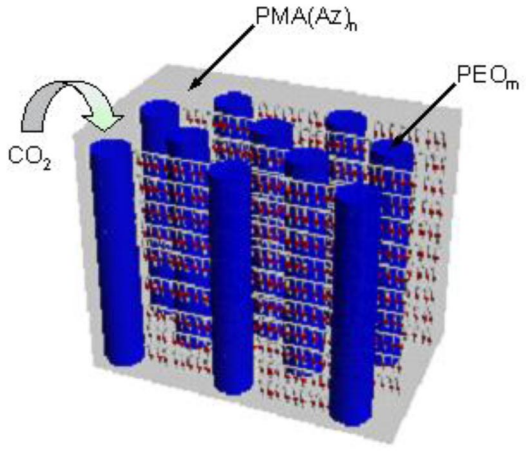

Fig. 7 Schematic representation of ordered periodic hexagonal-packed PEO cylinders formed in the PMA domain while CO_2 enters in PEO cylinders.

Remarkably, the transition entropy ΔS_{tr} decreases with increasing pressure, when the pressurizing fluid is Hg; this is typically the manifestation of a pure hydrostatic effect which restricts molecular motions under inert Hg. In complete contrast, ΔS_{tr} increases when the pressure is exerted by N_2 and CO_2. In this respect, as observed above, N_2 is a "neutral" fluid as compared to "chemically active" CO_2, and consequently the large increase of ΔS_{tr} shows that the organization of nanostructures is the easiest the more "active" is the fluid, in particular when the fluid is in supercritical state [32–34]. The influence of the pressure-transmitting fluid on the transition entropy at the interface is well illustrated by the increase of the Clapeyron slope $(dT/dp)_{tr}$ in the sequence $Hg < N_2 < CO_2$ as shown Fig. 8. Furthermore, the strong influence of supercritical CO_2 on the transition is spectacularly demonstrated by the significant shift of the isentropic transition temperature T_{iso} to lower temperatures.

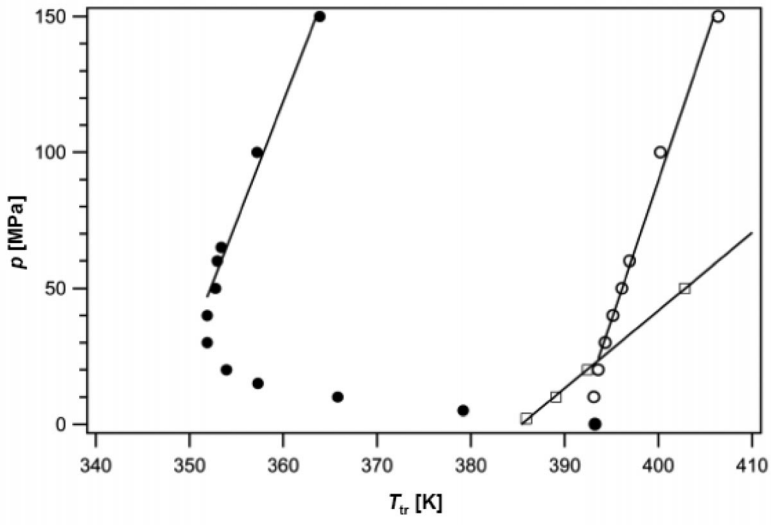

Fig. 8 Relation between the temperature of the isotropic temperature and pressure [34]. The different straight lines represent the Clapeyron slope depending on the pressure transmitting fluid: CO_2, filled circles; N_2, open circles; Hg, open squares. Note the significant shift of the transition temperature by CO_2.

CONCLUSION

An experimental set-up coupling a VW detector and a *pVT* technique has been used to simultaneously evaluate the amount of gas entering a polymer under controlled temperature and pressure and the concomitant swelling of the polymer. Scanning transitiometry has been used to determine the interaction energy during gas sorption in different polymers; the technique was also advantageously used to determine the thermophysical properties (i.e., isobaric thermal expansivity) of polymers submitted to gas sorption. Scanning transitiometry has also been used to evaluate the thermodynamic control of the formation of nanostructures in amphiphilic di-block copolymers. As a matter of fact, the striking effect of gas sorption is particularly observed when the gas is in supercritical state depending on thermodynamic conditions. The main conclusion is that a rigorous thermodynamic approach is the key for tuning molecular organizations in the nanoscale domain.

ACKNOWLEDGMENTS

The authors are grateful to the Japan Science and Technology (JST) Agency for support of this research through the CREST Project. S.A.E.B. gratefully acknowledges the financial support of JST-CREST program during her stay at the Tokyo Metropolitan University and also thanks the following organizations for their support, the French Institute of Petroleum and ARMINES-MINES ParisTech. T.Y. gratefully acknowledges the financial support from the Collège Doctoral Franco-Japonais during his stay at the University Blaise Pascal.

REFERENCES

1. S. A. E. Boyer, J.-P. E. Grolier. *Polymer* **46**, 3737 (2005).
2. B. Dewimille, J. Martin, J. Jarrin. *J. Phys. IV* **3**, 1559 (1993).
3. J. Jarrin, B. Dewimille, E. Devaux, J. Martin. *J. Int. SPE* **28482**, 203 (1994).
4. N. Von Solms, N. Zecchin, A. Rubin, S. I. Andersen, E. H. Stenby. *Eur Polym. J*. **41**, 341 (2005).
5. P. K. Mukherjee, S. J. Rzoska. *Phys. Rev. E* **65**, 051705 (2002).
6. Y. Maeda, T. Niori, J. Yamamoto, H. Yokokawa. *Thermochim. Acta* **57**, 428 (2005).
7. R. Triolo, A. Triolo, F. Triolo, D. C. Steytler, C. A. Lewis, R. K. Heenan, G. D. Wignall, J. M. DeSimone. *Phys. Rev. E* **61**, 4640 (2000).
8. Y. Kawabata, M. Nagao, H. Seto, S. Komura, T. Takeda, D. Schwahn, N. L. Yamada, H. Nobutou. *Phys. Rev. Lett*. **92**, 056103 (2004).
9. A. Seeger, D. Freitag, F. Freidel, G. Luft. *Thermochim. Acta* **424**, 175 (2004).
10. D. Y. Ryu, J. L. Lee, J. K. Kim, K. A. Lavery, T. P. Russell, Y. S. Han, B. S. Seong, C. H. Lee, P. Thiyagarajan. *Phys. Rev. Lett*. **90**, 235501 (2003).
11. I. W. Hamley. In *The Physics of Block Copolymers*, Oxford University Press, Oxford (1998).
12. M. W. Masten, F. S. Bates. *Macromolecules* **29**, 1091 (1996).
13. M. Lazzari, M. A. López-Quintela. *Adv. Mater*. **15**, 1583 (2003).
14. M. Aizawa, J. M. Buriak. *J. Am. Chem. Soc*. **128**, 5877 (2006).
15. Y. Tian, K. Watanabe, X. Kong, J. Abe, T. Iyoda. *Macromolecules* **35**, 3739 (2002).
16. H. Yoshida, K. Watanabe, R. Watanabe, T. Iyoda. *Trans. Mater. Res. Sci. Jpn*. **29**, 861 (2004).
17. K. Watanabe, Y. Tian, H. Yoshida, S. Asaoka, T. Iyoda. *Trans. Mater. Res. Sci. Jpn*. **28**, 553 (2003).
18. K. Watanabe, H. Yoshida, K. Kamata, T. Iyoda. *Trans. Mater. Res. Sci. Jpn*. **30**, 377 (2005).
19. R. Watanabe, T. Iyoda, T. Yamada, H. Yoshida. *J. Therm. Anal. Cal*. **85**, 713 (2006).
20. S. Y. Jung, T. Yamada, H. Yoshida, T. Iyoda. *J. Therm. Anal. Cal*. **81**, 563 (2005).
21. S. Hilic, A. A. H. Padua, J.-P. E. Grolier. *Rev. Sci. Instrum*. **71**, 4236 (2000).

22. S. Hilic, S. A. E. Boyer, A. A. H. Padua, J.-P. E. Grolier. *J. Polym. Sci., Part B: Polym. Phys.* **39**, 2063 (2001).
23. S. A. E. Boyer, J.-P. E. Grolier. *Polymer* **46**, 3737 (2005).
24. S. L. Randzio. *Chem. Soc. Rev.* **25***,* 383 (1996).
25. S. L. Randzio. *Thermochim. Acta* **300**, 29 (1997).
26. S. L. Randzio, J.-P. E. Grolier, J. R. Quint. *Rev. Sci. Instrum.* **65**, 960 (1994).
27. S. L. Randzio, J.-P. E. Grolier, J. Zaslona, J. R. Quint. French Patent 91 09227.
28. S. L. Randzio, J.-P. E. Grolier. French Patent 97 15221.
29. <www.transitiometry.com>.
30. S. A. E. Boyer, M.-H. Klopffer, J. Martin, J.-P. E. Grolier. *J. Appl. Polym. Sci.* **103**, 1706 (2006).
31. L. Rodier-Renaud, S. L. Randzio, J.-P. E. Grolier, J. R. Quint, J. Jarrin. *J. Polym. Sci., Part B: Polym. Phys.* **34**, 1229 (1996).
32. S. A. E. Boyer, J.-P. E. Grolier, L. Pison, C. Iwamoto, H. Yoshida, T. Iyoda. *J. Therm. Anal. Cal.* **85**, 699 (2006).
33. S. A. E. Boyer, J.-P. E. Grolier, H. Yoshida, T. Iyoda. *J. Polym. Sci., Part B: Polym. Phys.* **45**, 1354 (2007).
34. T. Yamada, S. A. E. Boyer, T. Iyoda, H. Yoshida, J.-P. E. Grolier. *J. Therm. Anal. Cal.* **89**, 9 (2007).
35. T. Yamada, S. A. E. Boyer, T. Iyoda, H. Yoshida, J.-P. E. Grolier. *J. Therm. Anal. Cal*. **89**, 717 (2007).